THE FASEB JOURNAL • RESEARCH • www.fasebj.org

TG101348, a selective JAK2 antagonist, ameliorates hepatic fibrogenesis *in vivo*

Büsra Öztürk Akcora,* Eshwari Dathathri,*,[1] Ana Ortiz-Perez,*,[1] Alexandros Vassilios Gabriël,*,[1] Gert Storm,*,† Jai Prakash,* and Ruchi Bansal*,‡,[2]

*Department of Biomaterials Science and Technology, Technical Medical Centre, Faculty of Science and Technology, University of Twente, Enschede, The Netherlands; †Department of Pharmaceutics, Utrecht Institute of Pharmaceutical Sciences, Faculty of Science, Utrecht University, Utrecht, The Netherlands; and ‡Department of Pharmacokinetics, Toxicology, and Targeting, Groningen Research Institute of Pharmacy, University of Groningen, Groningen, The Netherlands

ABSTRACT: Hepatic fibrosis, characterized by an excessive extracellular matrix (ECM) accumulation, leading to scar-tissue formation is a growing health problem worldwide. Hepatocellular damage due to liver injury triggers inflammation and transdifferentiation of quiescent hepatic stellate cells (HSCs) into proliferative, contractile, and ECM-producing myofibroblasts. Involvement of the Janus kinase (JAK)-2 pathway in the pathogenesis of fibrosis has been reported earlier. However, in this study, we have investigated the effect of selective JAK2 antagonist TG101348 in fibroblasts and inflammatory macrophages and *in vivo* in an acute carbon tetrachloride–induced liver injury mouse model. *In vitro*, TG101348 significantly inhibited TGF-β–induced collagen I expression in murine 3T3 fibroblasts. In human HSCs (LX2 cells), TG101348 potently attenuated TGF-β–induced contractility and the protein and gene expression of major fibrotic parameters (collagen I, vimentin, and α-smooth muscle actin). In LPS- and IFN-γ–stimulated inflammatory macrophages, TG101348 significantly reduced the NO release and strongly inhibited the expression of inflammatory markers (inducible nitric oxide synthase, C-C motif chemokine ligand 2, IL-1β, IL-6, and C-C chemokine receptor type 2). *In vivo* in an acute liver injury mouse model, TG101348 significantly attenuated collagen accumulation and HSC activation. Interestingly, TG101348 drastically inhibited macrophage infiltration and intrahepatic inflammation. Pharmacological inhibition of the JAK2 signaling pathway in activated HSCs and inflammatory macrophages using TG101348 suggests a potential therapeutic approach for the treatment of liver fibrosis.—Akcora, B. O., Dathathri, E., Ortiz-Perez, A., Gabriël, A. V., Storm, G., Prakash, J., Bansal, R. TG101348, a selective JAK2 antagonist, ameliorates hepatic fibrogenesis *in vivo*. FASEB J. 33, 9466–9475 (2019). www.fasebj.org

KEY WORDS: myofibroblasts · inflammatory macrophages · liver fibrosis · intrahepatic inflammation

Liver fibrosis is a condition causing scarring of tissue as a response to liver injury. It is a dynamic process that is characterized by excessive deposition of extracellular matrix (ECM), activation of hepatic stellate cells (HSCs), distortion of the hepatic vascular structure, and inflammatory cell infiltration (1, 2). Persistent liver injuries ultimately culminate in cirrhosis and end-stage liver failure and often require liver transplantation. As a response to hepatocellular injury, HSCs are activated and transdifferentiate into ECM-producing contractile myofibroblast-like cells that play a crucial role in the pathogenesis of hepatic fibrosis (3, 4). Activated HSCs play a multifaceted role during liver injury. HSCs produce ECM, and aggravate liver inflammation and angiogenesis *via* paracrine interactions (5).

Apart from HSCs, hepatic macrophages, a heterogeneous population of immune cells, play an important role in maintaining tissue homeostasis and in the progression and regression of chronic liver diseases (6–8). In the liver, macrophages undergo functional and phenotypic transformation in response to the cytokines and growth factors into classically activated proinflammatory M1 macrophages and alternatively activated restorative M2 macrophages (6–8). There is a continuous crosstalk between HSCs and macrophages during liver diseases (5, 9), which

ABBREVIATIONS: α-SMA, α-smooth muscle actin; 3D, 3-dimensional; ALT, alanine aminotransferase; ATCC, American Type Culture Collection; CCl_4, carbon tetrachloride; ECM, extracellular matrix; FBS, fetal bovine serum; FLT3, fms-like tyrosine kinase 3; GAPDH, glyceraldehyde 3-phosphate dehydrogenase; HSC, hepatic stellate cell; iNOS, inducible nitric oxide synthase; JAK, Janus kinase; MHC-II, major histocompatibility complex class II; NASH, nonalcoholic steatohepatitis; RET, rearranged during transfection; STAT, signal transducer and activator of transcription

[1] These authors contributed equally to this work.

[2] Correspondence: Department of Biomaterials, Science, and Technology, Technical Medical Centre, Faculty of Science and Technology, University of Twente, Drienerlolaan 5, 7522 NB Enschede, The Netherlands. E-mail: r.bansal@utwente.nl

doi: 10.1096/fj.201900215RR

This article includes supplemental data. Please visit *http://www.fasebj.org* to obtain this information.

0892-6638/19/0033-9466 © FASEB

implies that combined therapies targeting both HSCs and macrophages or HSC-macrophage crosstalk will be an effective approach for the treatment of hepatic fibrosis.

The Janus kinase (JAK) signal transducers and activators of transcription (STAT) pathway plays a critical role in the regulation of several crucial processes, including cell growth, differentiation, proliferation, and immune functions (10). In the liver, the JAK2 pathway is activated by growth hormone, cytokines (IFN-γ, IL-4, IL-6, IL-12, and IL-13), and leptin (11). The involvement of the JAK2 pathway in the pathogenesis of fibrosis (12, 13), hepatic steatosis (14, 15), ischemia-reperfusion injury (16), and hepatocellular carcinoma (17–19) has been documented earlier. JAK2 acts *via* the STAT-dependent or STAT-independent pathway in the HSCs. Studies have focused on the role of JAK2-induced pathways in hepatocytes and HSCs, whereas the JAK2 pathway and its implication in macrophages during liver injury has not been explored yet. Furthermore, TG101348, a selective JAK2 antagonist, has not been investigated in liver injury. Hence, in this study, we, for the first time, investigated the effect of TG101348 in fibroblasts and inflammatory macrophages *in vitro* and *in vivo* in an acute carbon tetrachloride (CCl_4)–induced liver injury mouse model.

MATERIALS AND METHODS

Cell lines

Human HSCs (LX2 cells), provided by Prof. Scott Friedman (Mount Sinai Hospital, New York, NY, USA), were cultured in DMEM-Glutamax (Thermo Fisher Scientific, Waltham, MA, USA) supplemented with 10% fetal bovine serum (FBS; Lonza, Basel, Switzerland) and antibiotics (50 U/ml penicillin and 50 μg/ml streptomycin; MilliporeSigma, Burlington, MA, USA). Human hepatocytes (HepG2) [American Type Culture Collection (ATCC), Manassas, VA, USA] and mouse NIH3T3 fibroblasts (ATCC) were cultured in DMEM (Lonza) supplemented with 2 mM L-glutamine (MilliporeSigma), 10% FBS (Lonza), and antibiotics (50 U/ml penicillin and 50 μg/ml streptomycin). Mouse RAW macrophages (ATCC) and human THP1 monocytes (ATCC) were cultured in FBS, L-glutamine, and antibiotics supplemented with Roswell Park Memorial Institute 1640 medium (Lonza). HUVECs were purchased from Lonza and cultured in endothelial basal medium (Lonza) supplemented with hydrocortisone, bovine brain extract, epidermal growth factor, gentamycin sulfate, amphotericin-B, and 10% fetal calf serum (Thermo Fisher Scientific).

Effects of JAK2 inhibitor TG101348 on mouse 3T3 fibroblasts and human LX2 cells

The JAK2 inhibitor TG101348 (Fedratinib) used in this study was purchased from Selleckchem (Houston, TX, USA). Cells were seeded in 24-well plates (5×10^4cells/well) or 12-well plates (1×10^5cells/well) and cultured overnight. To study the effects, cells were starved overnight with serum-free medium and incubated with starvation medium alone and 5 ng/ml of human recombinant TGF-β1 (Roche, Basel, Switzerland) with and without 5 μM TG101348. Cells (24-well plates) were then fixed with chilled acetone and methanol (1:1), dried, and stained for different markers (collagen I and vimentin) (antibodies are summarized in Supplemental Table S1). In addition, cells (12-well plates) were lysed with RNA lysis buffer to perform real-time quantitative PCR analyses or protein lysis buffer for Western blot analyses. Experiments were performed as 3 independent experiments.

Three-dimensional collagen I gel contraction assay

A 3-dimensional (3D) collagen I gel contraction assay was performed as previously described (5). Briefly, collagen suspension (5.0 ml) containing 3.0 ml Collagen G1 (5 mg/ml; Matrix Biosciences, Mörlenbach, Germany), 0.5 ml 10-times M199 medium, 85 μl 1N NaOH (MilliporeSigma), and sterile water was prepared and mixed with 1.0 ml (2×10^6) LX2 cells. The collagen-gel cells suspension (0.6 ml/well) was plated in a 24-well culture plate and allowed to polymerize for 1 h at 37°C. Polymerized gel was then incubated with 1 ml of serum-free medium with or without TGF-β (5 ng/ml) together with 5 μM TG101348 followed by detachment of the gels from the culture wells. Photographs were taken with a digital camera (Samsung ES10; Samsung, Seoul, South Korea) at 72 h. The size of the gels was digitally measured and normalized with their respective well size in each image. Gel contraction experiments were performed in duplicates as 3 independent experiments.

Effects of JAK2 inhibitor TG101348 on differentiated RAW macrophages

RAW macrophages were plated in 12-well plates (1×10^5 cells/well) and cultured overnight at 37°C and 5% CO_2. To assess the effects, cells were incubated with medium alone or M1 or inflammatory stimulus (10 ng/ml of murine IFN-γ and 10 ng/ml LPS) with or without TG101348 (0.5, 1.0, 5.0, and 10.0 μM) for 24 h. Cells were lysed with RNA lysis buffer to perform real-time quantitative PCR analyses or with protein lysis buffer for Western blot analyses. All the experiments were performed as 3 independent experiments.

Cytokine detection

Measurement of TNF-α and IL-6 in macrophage-conditioned medium was performed using ELISA kits according to the manufacturer's instructions (Thermo Fisher Scientific). Briefly, RAW macrophages were incubated with medium alone or M1 or inflammatory stimulus (10 ng/ml murine IFN-γ and 10 ng/ml LPS) with or without TG101348 (5.0 μM) for 24 h. The conditioned medium or culture supernatant was collected and stored at −80°C until use. This ELISA assay uses the quantitative sandwich immunoassay technique. By comparing the absorbance of the samples to the standard curve, the concentration of the cytokines in culture supernatant was determined.

Effects of JAK2 inhibitor TG101348 on NO release

The effect of TG101348 on M1 inflammatory macrophages was assessed by measuring the inhibition in nitrite NO_2 release, a stable NO metabolite produced by M1 inflammatory macrophages. RAW cells (2×10^5 cells/200 μl/well) seeded in 96-well plates were cultured with IFN-γ (10 ng/ml) and LPS (10 ng/ml) together with different concentrations of JAK2 inhibitor TG101348 (0, 0.5, 1, 5, and 10 μM). After 24 h, 100 μl culture supernatant was added to 100 μl of Griess reagent (1% sulfanilamide, 0.1% naphthylethylendiamine dihydrochloride, and 3% phosphoric acid), and absorbance at 540 nm was measured using a microplate reader.

Cell viability assay in human LX2 cells and mouse macrophages

To assess the effects on cell viability, cells were plated in 96-well plates and incubated with different concentrations of TG101348 (0.1, 0.5, 1.0, 2.5, 5, 10, and 25 μM) for 24 h. A cell viability assay was performed using Alamar Blue reagent (Thermo Fisher Scientific) as per the manufacturer's instructions. The results are represented as the percentage of cell viability normalized to untreated control cells (at 100%). All measurements were performed in triplicates from 3 independent experiments.

Animal experiments

All the animal experiments in this study were performed in strict accordance with the guidelines and regulations for the Care and Use of Laboratory Animals, Utrecht University, The Netherlands. The protocols were approved by the Institutional Animal Ethics Committee of the University of Twente, The Netherlands. Eight-week-old C57BL/6 male mice were purchased from Harlan Sprague-Dawley (Indianapolis, IN, USA) and kept in a 12-h light/dark cycle with *ad libitum* normal diet.

CCl_4-induced acute liver injury mouse model

To study the effect of TG101348, 8-wk-old male C57BL/6 mice were treated with a single intraperitoneal injection of olive oil or CCl_4 (1 ml/kg in olive oil) at d 1. At d 2 and 3, CCl_4-treated mice received an intraperitoneal administration of 5 mg/kg TG101348 prepared in 1% DMSO (MilliporeSigma) and 5% β-hydroxycyclodextrin (MilliporeSigma) or vehicle treatment (1% DMSO and 5% β-hydroxycyclodextrin and PBS) ($n = 5$ per group). At d 4, all mice were euthanized, and livers were harvested for the subsequent analysis.

In vitro human 3D spheroid nonalcoholic steatohepatitis model

To prepare the human 3D spheroids, human hepatocytes (HepG2) (80%), human monocytes (THP1) (10%), human HSCs (LX2) (5%), and HUVECs (5%) were mixed using complete medium containing 10% FBS. Spheroids containing 1200 total cells were plated in ultralow adhesion U-bottomed plates (1200 cells/100 μl) followed by addition of 100 μl of medium. After 7 d of culturing, 3D spheroids were incubated with 10 μg/ml LPS with and without TG101348 (25 μM). After 7 d of culturing, images of the 3D spheroids were captured using a light microscope, and spheroids were embedded in Tissue-Tek optimum cutting temperature embedding medium (Sakura Finetek, Torrance, CA, USA), fixed, and snap frozen in 2-methyl butane chilled on dry ice. The spheroids were cryosectioned into 4-μm cryosections and stained as described below.

Immunohistochemistry

Liver tissues were harvested, transferred to Tissue-Tek optimum cutting temperature embedding medium, and snap frozen in 2-methyl butane chilled on dry ice. Cryosections (4 μm) were cut using a Leica CM 3050 cryostat (Leica Microsystems, Buffalo Grove, IL, USA). The sections were air dried and fixed with acetone for 10 min. Cells or tissue sections were rehydrated with PBS and incubated with the primary antibody (refer to Supplemental Table S1) for 1 h at room temperature. Cells or sections were then incubated with horseradish peroxidase–conjugated secondary antibody for 1 h at room temperature, then incubated with horseradish peroxidase–conjugated tertiary antibody for 1 h at room temperature. Thereafter, peroxidase activity was developed using a 3-amino-9-ethyl carbazole substrate kit (Thermo Fisher Scientific) for 20 min, and nuclei were counterstained with hematoxylin (MilliporeSigma). For liver sections, endogenous peroxidase activity was blocked by 3% H_2O_2 prepared in methanol. Cells or sections were mounted with Aquatex mounting medium (Merck, Darmstadt, Germany). The staining was visualized, and the images were captured using light microscopy (Nikon Eclipse E600 microscope; Nikon, Tokyo, Japan). Furthermore, sections were scanned using a Hamamatsu NanoZoomer Digital slide scanner 2.0-HT (Hamamatsu, Hamamatsu City, Japan) for quantitative histologic analysis. High-resolution scans were viewed using NanoZoomer Digital Pathology viewer software (Hamamatsu). About 20 images (×100) of each entire section (from NanoZoomer Digital Pathology) were imported into ImageJ and were analyzed quantitatively at a fixed threshold. All the primary antibodies used in this study have been pretested for specificity. The stainings performed in the study included the negative control (without primary antibody) to confirm the specificity of the staining and showed no nonspecific staining (unpublished results). Oil Red O staining was performed using Oil Red O staining kit (MilliporeSigma) as per the manufacturer's instructions.

Western blot analysis

Cells were lysed using standard Western blot lysis buffer (Thermo Fisher Scientific), and the prepared cell lysates were stored at −80°C until use. The samples were boiled and subjected to SDS-PAGE with 10% Tris glycine gels (Thermo Fisher Scientific) followed by protein transfer onto a PVDF membrane. The membranes were developed according to the standard protocols using primary and secondary antibodies as mentioned in Supplemental Table S2. The bands were visualized using ECL detection reagent (PerkinElmer, Waltham, MA, USA) and photographed using a FluorChem M Imaging System (ProteinSimple; San Jose, CA, USA). Intensity of individual bands was quantified using ImageJ densitometry software and expressed in relative percentage.

RNA extraction, RT, and real-time quantitative PCR

Total RNA from cells and liver tissues was isolated using a GenElute Total RNA Miniprep Kit (MilliporeSigma) and an SV Total RNA Isolation System (Promega, Madison, WI, USA), respectively, according to the manufacturer's instructions. The RNA concentration was quantitated by a UV spectrophotometer (Thermo Fisher Scientific). Total RNA (1 μg) was reverse transcribed using an iScript cDNA Synthesis Kit (Bio-Rad, Hercules, CA, USA). All the primers were purchased from MilliporeSigma. Real-time PCR was performed using 2-times SensiMix Sybr and Fluorescein Kit (QT615-05; Meridian Life Science, Memphis, TN, USA), 20 ng cDNA, and pretested gene-specific primer sets (listed in Supplemental Tables S3 and S4). The cycling conditions for the Bio-Rad CFX384 Real-Time PCR detection system were 95°C for 10 min, 40 cycles of 95°C/15 s, 58°C/15 s, and 72°C/15 s. Finally, C_t values were normalized to reference gene glyceraldehyde 3-phosphate dehydrogenase (GAPDH), and fold changes in expression were calculated using the $2^{-\Delta\Delta Ct}$ method.

Transcriptomic mRNA-expression analysis in the human liver tissues

JAK2, collagen I, and α-smooth muscle actin (α-SMA) mRNA expression was assessed in the publicly available transcriptome

datasets of liver tissue from patients with fibrosis (GSE14323) (20) obtained from the National Center for Biotechnology Information Gene Expression Omnibus database (*http://www.ncbi.nlm.nih.gov/geo*). Patients were categorized into 2 groups, normal ($n = 19$) and cirrhosis ($n = 41$), and data were analyzed using the online database Gene Expression Omnibus.

Statistical analyses

All the data are presented as means ± SEM. The graphs and statistical analyses were performed using Prism v.5.02 (GraphPad Prism Software, La Jolla, CA, USA). Comparisons with the control group were analyzed using unpaired Students' t test, whereas multiple comparisons between different groups were performed by 1-way ANOVA with Bonferroni posthoc test. The differences were considered significant at $P < 0.05$. Correlation was performed using nonparametric Spearman correlative analysis with Gaussian approximation. The dot plots for the correlation were generated using GraphPad Prism and represented with Spearman r and 2-tailed P value.

RESULTS

Up-regulation of JAK2 in patients with human cirrhosis

Liver fibrosis is characterized by increased expression of collagen I as a major ECM protein and α-SMA indicating stellate cell activation and are reported to be the markers for assessing the extent of liver damage (14, 15). The expression of JAK2, collagen I, and α-SMA were analyzed in different patients with cirrhosis using transcriptomic analysis. We observed significantly increased expression levels of JAK2 (**Fig. 1*A***) concomitant with induced collagen I and α-SMA expression in human cirrhotic livers as compared with normal livers (Fig. 1*B*, *C*). We performed a correlative analysis between JAK2 and collagen I expression to demonstrate the direct correlation of JAK2 expression with fibrosis. We found a highly significant correlation between JAK2 and collagen I expression as shown in Fig. 1*D* (Spearman $r = 0.6157$, $P < 0.0001$). These correlations suggest the strong association between the JAK2 signaling pathway and development of liver fibrosis.

Inhibition of JAK2 signaling pathway using JAK2 inhibitor TG101348 inhibited TGF-β–induced mouse 3T3 fibroblasts activation

To understand the role of the JAK2 pathway in fibrosis and fibroblasts activation, we first analyzed JAK2 expression in TGF-β–activated mouse 3T3 fibroblasts. The cytokine TGF-β1 activates fibroblasts, mediates tissue repair and wound healing, and has been implicated in liver diseases (21, 22). Therefore, we used TGF-β to activate fibroblasts. We observed increased expression of major fibrotic parameters (*i.e.*, collagen I, α-SMA, and desmin) upon TGF-β activation, along with significantly high expression of JAK2 (**Fig. 2*A***). To study the functional significance of JAK2 in fibroblasts activation, we treated TGF-β–activated 3T3 fibroblasts with TG101348, a selective JAK2 inhibitor. We observed increased protein expression of collagen I in

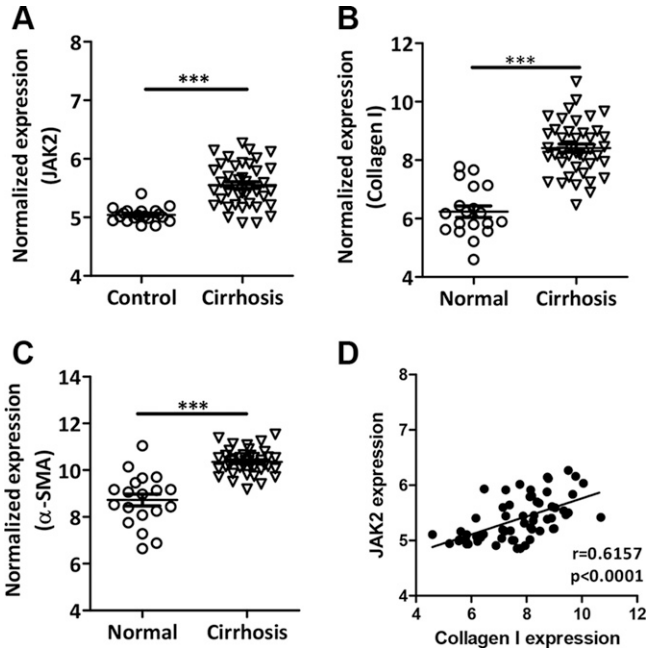

Figure 1. Up-regulation of JAK2 expression in patients with liver cirrhosis. Normalized intrahepatic expression of JAK2 (*A*), collagen I (*B*), and α-SMA (*C*) and correlative analysis of JAK2 and collagen I expression (*D*) from patients with cirrhosis: control ($n = 19$) and cirrhosis ($n = 41$). *r*, Spearman coefficient; *p*, 2-tailed *P* value calculated using nonparametric Spearman correlative analysis with Gaussian approximation. Data are presented as means ± SEM. ***$P < 0.001$ denotes significance *vs.* control.

3T3 fibroblasts upon TGF-β activation, and this increased collagen I expression was strongly attenuated following treatment with JAK2 inhibitor, suggesting the important role of the JAK2 pathway in TGF-β–induced fibroblasts activation (Fig. 2*B*).

TG101348 inhibited the activation and contractility of human LX2 cells *in vitro*

We further studied the effect of the JAK2 inhibitor TG101348 in immortalized human HSCs (LX2). We first analyzed the inhibition of the JAK2 signaling pathway using Western blot analysis. We observed that phosphorylated (p) JAK2 protein expression was significantly induced following TGF-β–induced LX2 activation, which was strongly reduced following treatment with TG101348 (Supplemental Fig. S1). Furthermore, nonphosphorylated JAK2 expression was also decreased after treatment with TG101348. JAK enzymes usually signal through STATs; therefore, we analyzed whether JAK2 inhibition is reflected in changes in one of the STAT factors (*i.e.*, STAT5) (23). Indeed, we observed that JAK2 pathway inhibition led to the significant reduction in STAT5 phosphorylation (Supplemental Fig. S1).

Following TGF-β activation, we observed a highly significant increase in the protein expression levels of collagen I (major ECM and fibrosis marker), vimentin (mesenchymal cell and HSCs activation marker), and α-SMA (HSCs activation marker) (**Fig. 3*A***). On inhibition of the JAK2 pathway, we observed a substantial reduction in the

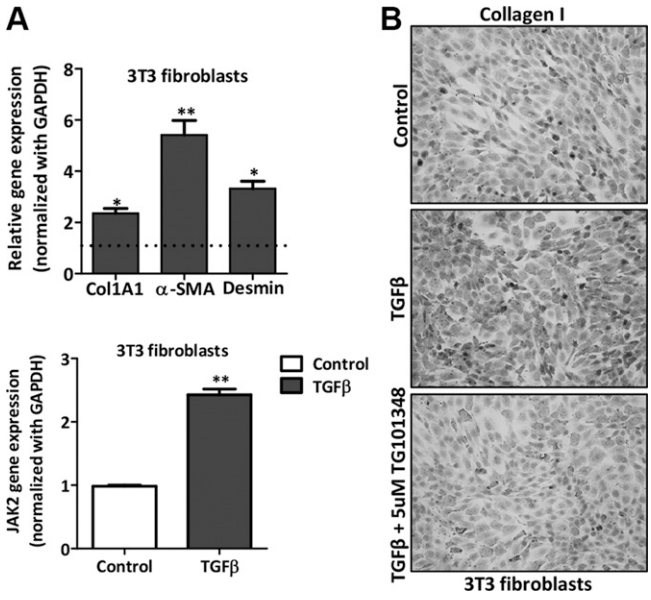

Figure 2. Inhibitory effect of TG101348 on TGF-β–activated 3T3 fibroblasts. *A*) Normalized relative gene expression of collagen I, α-SMA, desmin, and JAK2 in mouse 3T3 fibroblasts with and without TGF-β activation. Dashed line represents the expression levels in control (non-TGF-β) 3T3 fibroblasts. *B*) Representative images (×20 magnification) of collagen I protein staining in control and TGF-β (5 ng/ml)–activated 3T3 fibroblasts with and without treatment with JAK2 antagonist TG101348 (5 μM). $*P < 0.05$, $**P < 0.01$ denotes significance *vs.* TGF-β–activated 3T3 fibroblasts.

protein expression of collagen I, vimentin, and α-SMA as seen in the immunostainings (Fig. 3*A*). The increased protein expression was paralleled by mRNA expression, whereby incubation with TGF-β triggered the increased expression of mRNA transcripts of collagen I, α-SMA, and vimentin, whereas treatment with TG101348 completely attenuated the expression of these fibrosis-specific parameters (Fig. 3*B*). During fibrogenesis, HSCs migrate to the site of tissue injury and differentiate into contractile myofibroblasts that contribute to liver stiffness (4). Hence, we further examined the effect of TG101348 on the contractility of LX2 cells using the 3D collagen-gel contraction assay. We observed that TG101348 strikingly reduced the TGF-β–induced contractility after 72 h (Fig. 3*C, D*). Overall, these results further confirm the significance of the JAK2 pathway in TGF-β–induced activation and contractility of human HSCs.

JAK2 signaling pathway inhibits LPS- and IFN-γ–induced M1 polarization

We then investigated the role of the JAK2 signaling pathway in differently polarized macrophages. We first examined the expression of JAK2 in unpolarized control M0 macrophages, LPS- and IFN-γ–induced proinflammatory M1 macrophages, and IL-4– and IL-13–induced restorative M2 macrophages. We found increased JAK2 expression in M1 polarized macrophages, suggesting the role of the JAK2 signaling pathway in inflammation (**Fig. 4*A***). We also analyzed the inhibition of the JAK2 signaling pathway using Western blot analysis. We observed that pJAK2 protein expression was significantly increased in M1-differentiated macrophages and was reduced following treatment with TG101348 (Supplemental Fig. S2). However, we did not find any significant differences in the nonphosphorylated JAK2 protein expression after treatment with TG101348. We then also analyzed the expression of pSTAT5 and observed inhibition in pSTAT5 expression after treatment with TG101348, suggesting that JAK2 signals *via* the downstream STAT5 signaling pathway (Supplemental Fig. S2).

We further found that TG101348 substantially reduced M1 polarization, as depicted in M1-specific proinflammatory signature markers [*i.e.*, inducible nitric oxide synthase (iNOS) or nitric oxide synthase 2 (NOS2), IL-6, IL-1β, C-C motif chemokine ligand 2 or monocyte chemoattractant protein 1, and C-C chemokine receptor type 2] (Fig. 4*B–F*). Furthermore, treatment with JAK2 inhibitor TG101348 dose-dependently inhibited the M1-induced NO release (an indicator of M1 activation) (Fig. 4*G*) and inflammatory cytokines (TNF-α and IL-6) secretion (Fig. 4*H, I*). Interestingly, at these doses, no effect on the cell viability of macrophages was observed.

JAK2 signaling pathway inhibition ameliorates fibrogenesis *in vivo* in acute liver injury mouse model

Finally, we studied the effects of TG101348 on the fibrogenesis *in vivo* in an acute liver injury mouse model. Acute liver injury *via* intraperitoneal administration of CCl_4 resulted in an increased intrahepatic protein expression of collagen I and collagen III protein expression in comparison with the olive oil–administered control livers, as shown in the microscopic images and quantitative staining analysis (**Fig. 5**). Strikingly, *in vivo* postdisease treatment with TG101348 considerably attenuated collagen I and collagen III expression (Fig. 5). We also assessed the effect of TG101348 on the HSCs activation in a CCl_4-induced liver injury mouse model. A significant increase in the HSCs activation was observed in the fibrotic mice as compared with the olive oil–treated mice, as indicated by the higher levels of desmin protein (**Fig. 6**). After treatment with TG101348, a drastic decrease in the desmin levels was observed (Fig. 6). Overall, inhibition of the JAK2 pathway resulted in decreased collagen and desmin protein levels, contributing to down-regulation of HSC activation and amelioration of fibrogenesis *in vivo*. Although TG101348 is a selective and potent inhibitor of JAK2, it can also block other kinases [*e.g.*, fms-like tyrosine kinase 3 (FLT3) and rearranged after transfection (RET) as also reported previously (24)]. We have also analyzed the expression of FLT3 and RET tyrosine kinases in the CCl_4-induced acute liver injury mouse model. We observed no significant differences in FLT3 in the gene expression analysis. However, significant differences were observed in RET gene expression. RET expression was strongly increased during CCl_4-induced liver injury, which was significantly inhibited by TG101348, suggesting that TG101348 can inhibit FLT3 in addition to JAK2 (Supplemental Fig. S3).

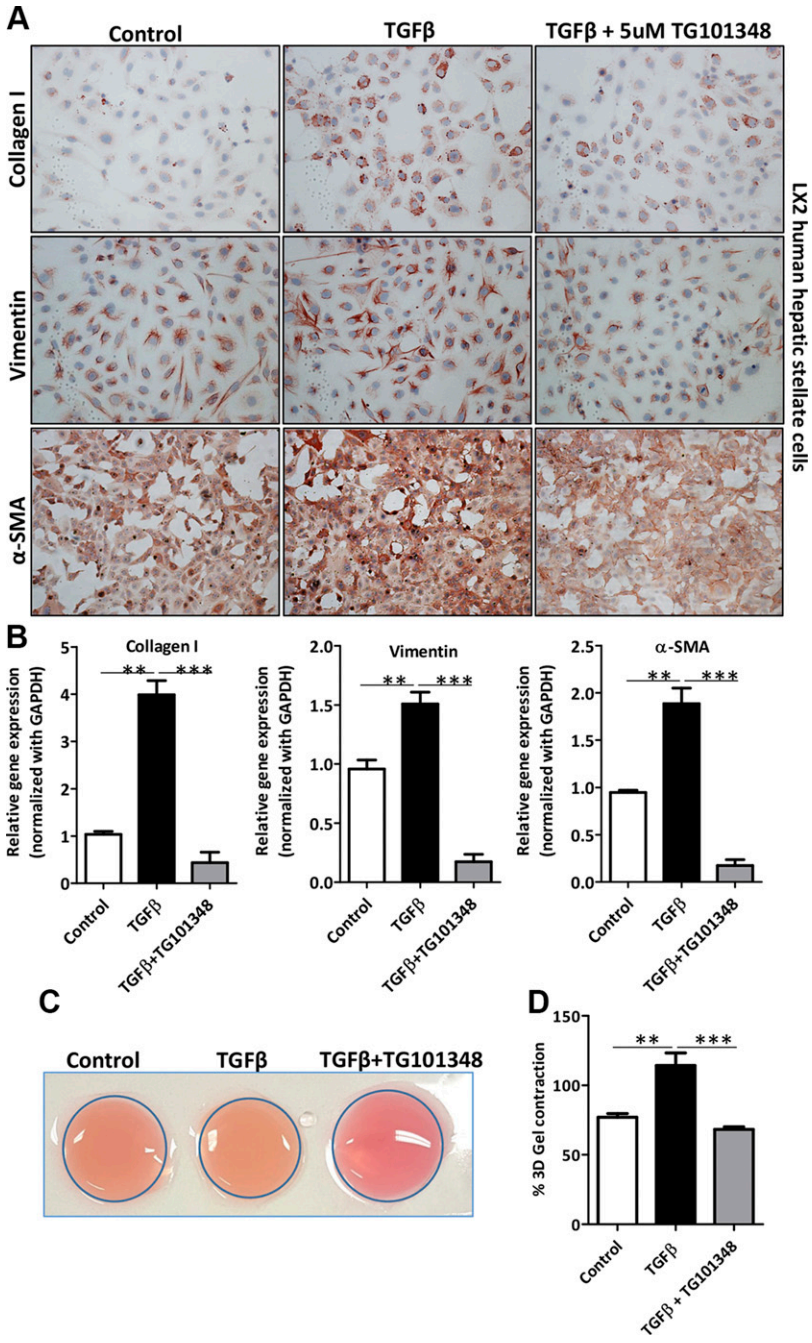

Figure 3. TG101348 inhibits TGF-β–induced activation and contractility of human HSCs (LX2 cells). *A*) Representative images (×20 magnification) of collagen I–, vimentin-, and α-SMA–stained control human HSCs (LX2 cells) and TGF-β (5 ng/ml)–activated human HSCs with and without treatment with 5 μM TG101348. *B*) Quantitative gene expression (normalized with GAPDH) of fibrotic parameters: collagen I, α-SMA, and vimentin. *C*, *D*) Representative images (*C*) and quantitative analysis (*D*) (expressed in %) of 3D collagen I gel contraction (after 72 h of incubation) of LX2 cells (control) and TGF-β–activated LX2 cells treated with or without TG101348 (5 μM). $^{**}P < 0.01$, $^{***}P < 0.001$ denote significance.

JAK2 signaling pathway inhibition attenuates liver inflammation in acute liver injury mouse model

We further investigated the effects of the inhibitor TG101348 on the macrophage infiltration and macrophage polarization *in vivo.* During CCl_4-induced acute liver injury, we observed significant intrahepatic infiltration or *de novo* intrahepatic proliferation of macrophages as confirmed by F4/80 [also called EMR1 (EGF-like module-containing mucin-like hormone receptor-like 1, a pan macrophage marker)] immunostainings. Furthermore, we found increased macrophage activation as assessed by major histocompatibility complex class II (MHC-II) staining and iNOS gene expression (**Fig. 7*A, B***) and decreased M2 restorative macrophages as confirmed by β-N-acetyl hexosaminidase immunostainings and arginase I gene expression in the livers of CCl_4-treated animals as compared with normal livers from control olive oil–treated animals (Fig. 7*A, B*). Interestingly, TG101348 inhibited macrophage infiltration (reduced F4/80 expression), reduced macrophage activation (M1 polarization) in agreement with our *in vitro* results, and increased M2 restorative macrophages (Fig. 7*A, B*), shifting the M1-M2 balance toward M2, eventually resulting in reduced liver inflammation and hence amelioration of fibrosis. We also measured alanine aminotransferase (ALT) levels in the serum and found inhibition in liver injury–induced ALT levels, further suggesting TG101348 significantly improved the liver function (Fig. 7*C*).

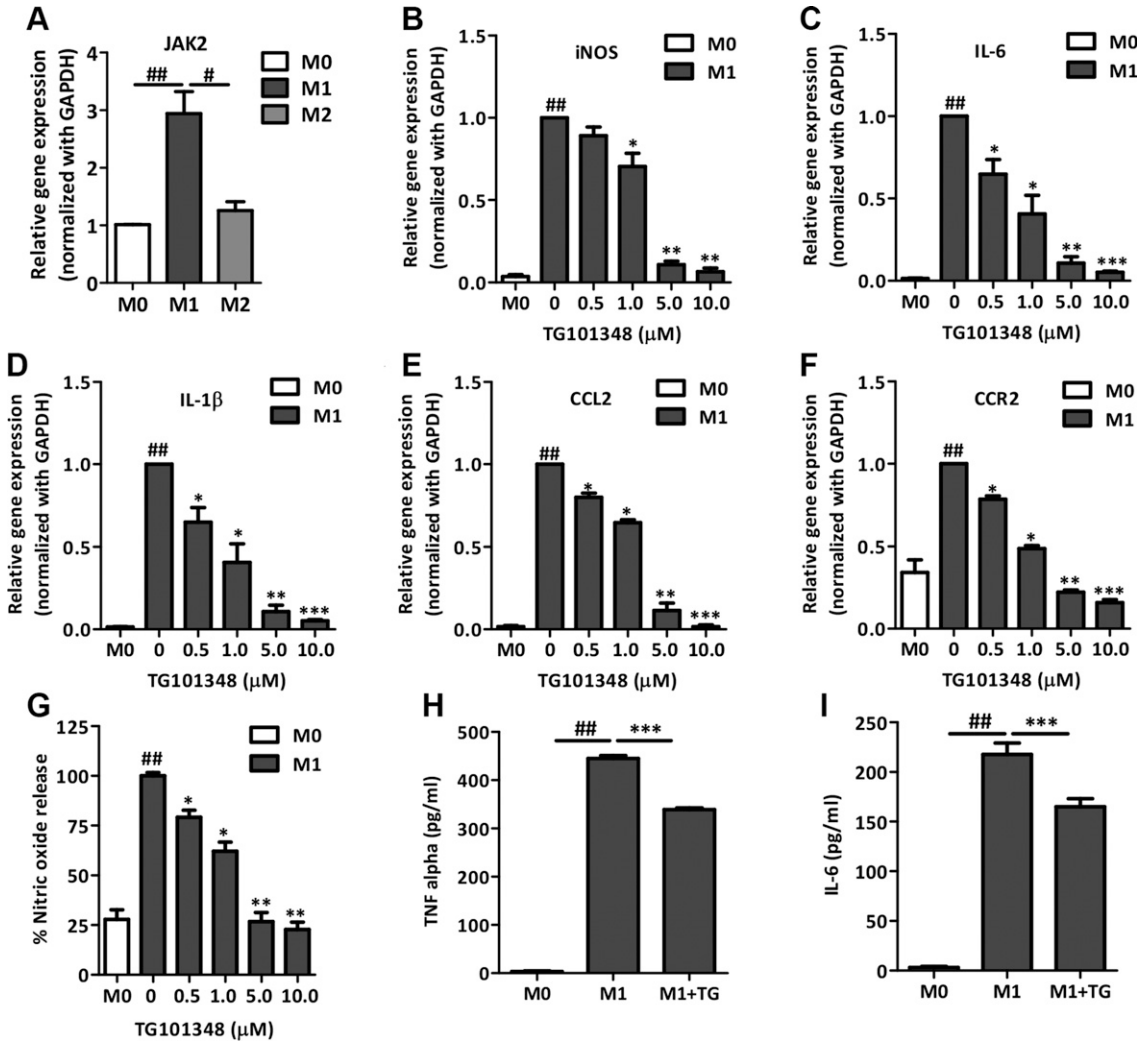

Figure 4. JAK2 antagonist TG101348 inhibits NO release and gene expression of inflammatory markers in LPS- and IFN-γ–stimulated mouse RAW macrophages. *A*) Relative gene expression of JAK2 in M0 (control), M1 (LPS- and IFN-γ–treated), and M2 (IL-4– and IL-13–treated) macrophages. *B–F*) Relative gene expression (normalized with GAPDH) of iNOS (*B*), IL-6 (*C*), IL-1β (*D*), C-C motif chemokine ligand 2 (CCL2) (*E*), and C-C chemokine receptor type 2 (CCR2) (*F*) assessed in RAW cells incubated with medium alone (M0) or M1 stimulus (10 ng/ml LPS and 10 ng/ml IFN-γ) with TG101348 (0, 0.5, 1, 5 and 10 μM). *G–I*) NO release (expressed in %) (*G*) and cytokine TNF-α (*H*) and IL-6 (*I*) as analyzed in the culture supernatant of RAW 264.7 cells incubated with medium alone (M0) or M1 stimulus (10 ng/ml LPS and 10 ng/ml IFN-γ) with TG101348 (0, 0.5, 1, 5 and 10 μM). $^{\#}P < 0.05$, $^{\#\#}P < 0.01$ denotes significance *vs.* control or M2 macrophages. $^{*}P < 0.05$, $^{**}P < 0.01$, $^{***}P < 0.001$ denotes significance *vs.* M1-differentiated macrophages.

Although we have not examined the therapeutic efficacy of TG101348 in advanced liver cirrhosis, considering the increased JAK2 expression in human cirrhosis and multidimensional beneficial effects of TG101348 as observed in this study, we speculated that TG101348 can be of great potential for the treatment of chronic cirrhosis. To further extrapolate our findings, we tested TG101348 in a 3D human spheroids–based *ex vivo* nonalcoholic steatohepatitis (NASH) model in which 3D human spheroids were formed from human hepatocytes (HepG2), human HSCs (LX2), human monocytes (THP1), and HUVECs. Patients with NASH have demonstrated increased hepatic endotoxin levels (*e.g.*, LPS, possibly derived from the gut). These pathogen-associated molecular patterns (*e.g.*, LPS derived from the gut) have shown to contribute to insulin resistance and interact with hepatic TLR, inducing an inflammatory response (25). Because of the existing evidences supporting LPS involvement during NASH, we treated the spheroids with LPS to mimic the human NASH. LPS-treated 3D spheroids were then incubated with TG101348 to investigate the effect of JAK2 inhibition in NASH. We observed that incubation of spheroids with LPS led to the increased Oil Red O staining (steatosis), collagen I expression, and MHC-II expression. These induced parameters were reduced significantly following treatment with TG101348 (Supplemental Fig. S4).

DISCUSSION

In this study, we have investigated the therapeutic efficacy of selective JAK2 antagonist TG101348 in fibroblasts and

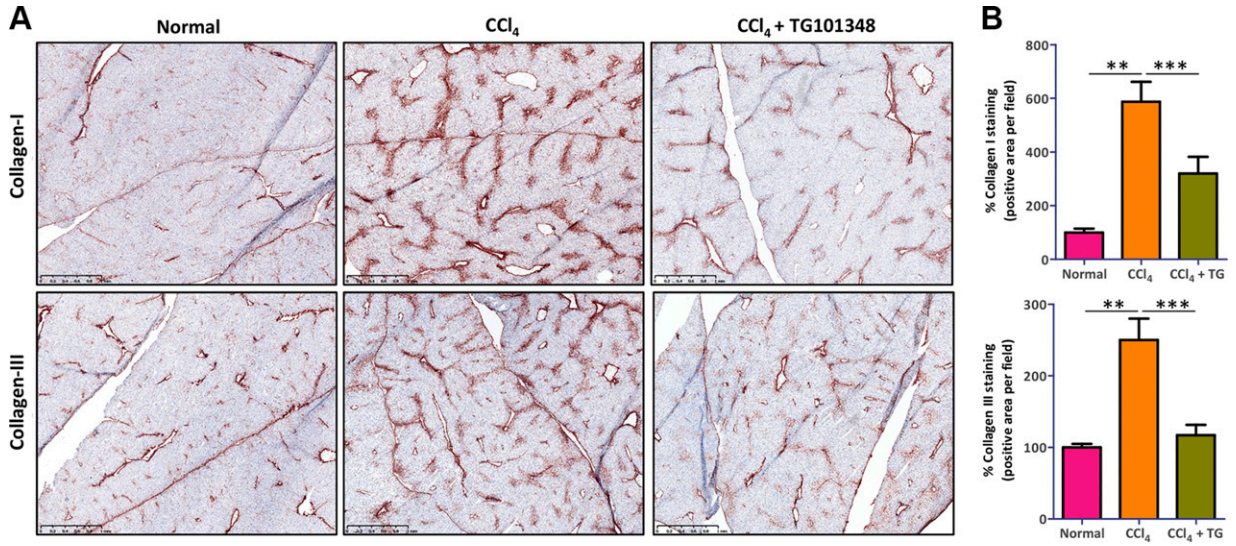

Figure 5. JAK2 inhibitor TG101348 (TG) ameliorates fibrogenesis in acute CCl_4-induced liver injury mouse model. Representative photomicrographs (*A*) and quantitative analysis (*B*) of collagen I– and collagen III–stained liver sections from normal CCl_4 mice and TG101348-treated CCl_4 mice. Scale bars, 1mm. $^{**}P < 0.01$, $^{***}P < 0.001$ denote significance.

inflammatory macrophages and *in vivo* in an acute CCl_4-induced liver injury murine model. We have shown that JAK2 is overexpressed in patients with human liver cirrhosis and in fibroblasts and inflammatory macrophages. Furthermore, we presented that TG101348, a highly selective JAK2 antagonist, inhibited HSCs activation, contractility, and inflammatory macrophages *in vitro* and *in vivo* in an acute liver injury mouse model.

During liver injury, HSCs and macrophages play the critical role in the progression of fibrosis (26). Therefore, simultaneous inhibition of these 2 key cell types is crucial for the regression of fibrosis. JAK2 overexpression on HSCs has been documented in liver cirrhosis (12). Furthermore, in another study, JAK2, rho guanine nucleotide exchange factor 1 (ARHGEF1), and rho-associated coiled-coil-containing protein kinase (ROCK) expression in HSCs has been associated with portal hypertension and decompensation in human cirrhosis (13). Our study corroborates with previous findings that inhibition of the JAK2 pathway using the highly selective JAK2 antagonist inhibits the activation and contractility of hepatic myofibroblasts. We also showed that the effects are mediated *via* the STAT5 signaling pathway, which corroborated with the previous findings (23).

However, we have also demonstrated the role of JAK2 in inflammation during liver injury. It has been previously shown in an ischemia-reperfusion injury mouse model that JAK2 signaling play a crucial role in inflammatory cell infiltration (16). Furthermore, researchers have demonstrated that the inhibition of JAK2 blunted the expression of the inflammatory signature markers (16). In line with the reported study, our results report the overexpression of JAK2 in LPS- and IFN-γ–stimulated proinflammatory M1 macrophages as compared with control and IL-4– and IL-13–stimulated restorative M2 macrophages. Furthermore, we have also demonstrated that JAK2 inhibition led to the reduced expression of inflammatory markers both *in vitro*. *In vivo*, we confirm that JAK2 inhibition ameliorated intrahepatic inflammation by reducing the sequestration of macrophages and inhibition of proinflammatory phenotypes while promoting the restorative phenotype, thereby promoting regression of liver injury.

In our opinion, the JAK2 pathway is overexpressed in HSCs and inflammatory macrophages and contributes to the aggravation of fibrogenesis. Previous studies have demonstrated the role of the JAK2 pathway in cirrhosis, ischemia-reperfusion liver injury, hepatocellular carcinoma, and steatohepatitis (12–18). However, the role of the JAK2 pathway in proinflammatory macrophages and inflammation remained largely unexplored and might be very interesting for developing inflammation-driven diseases, especially nonalcoholic fatty liver diseases and

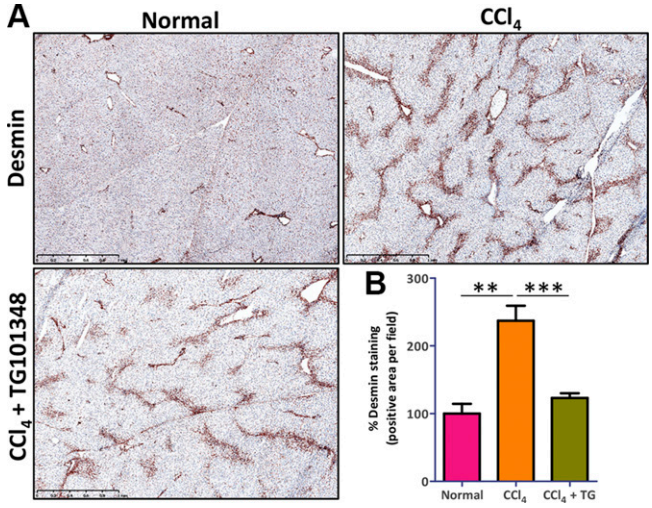

Figure 6. Inhibition of HSCs activation by JAK2 inhibitor TG101348 (TG) *in vivo* in acute CCl_4-induced liver injury mouse model. Microscopic images (*A*) and quantitative analysis (*B*) of desmin-stained liver sections from control mice and CCl_4-treated mice with and without TG101348. Scale bars, 1mm. $^{**}P < 0.01$, $^{***}P < 0.001$ denote significance.

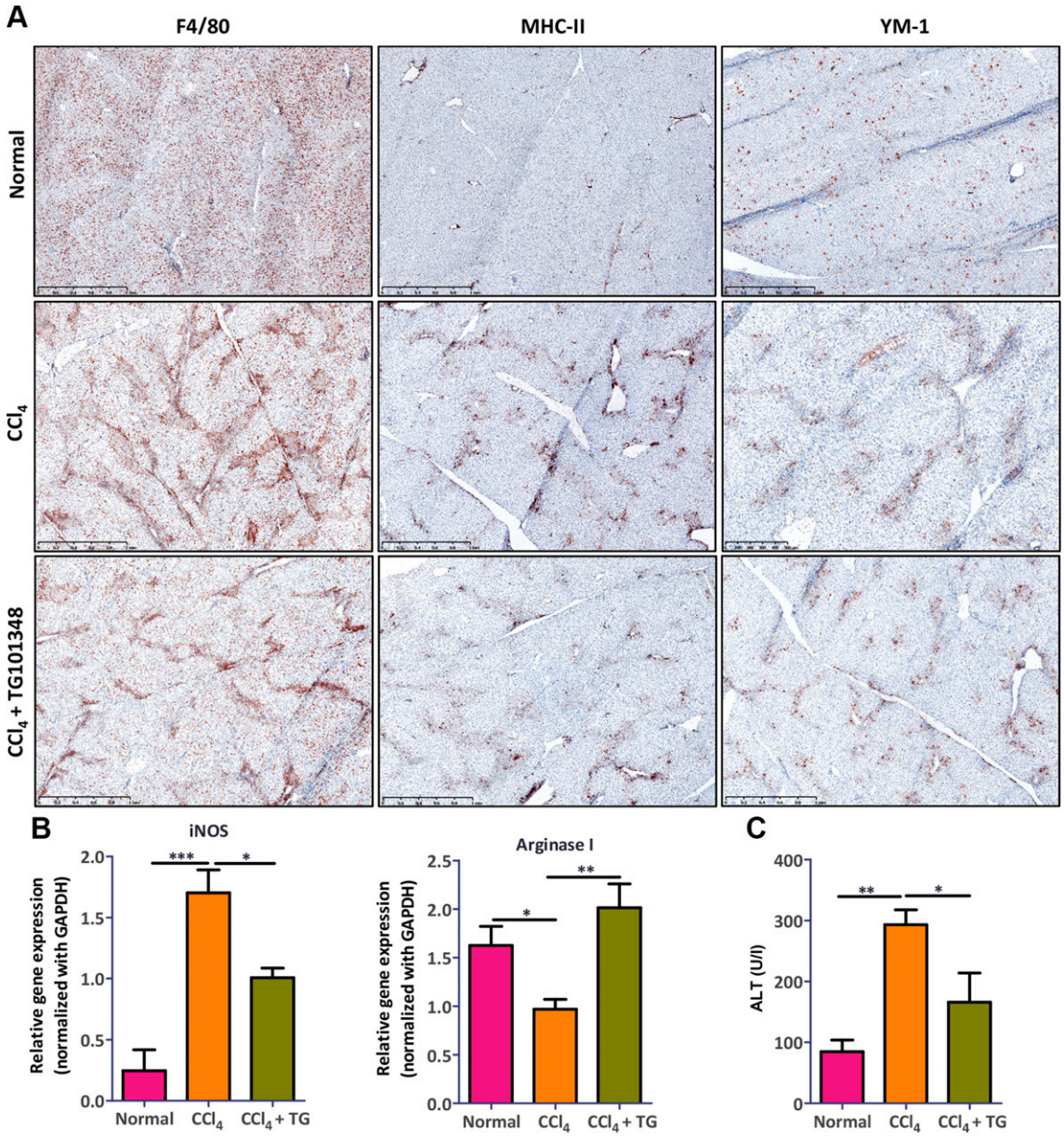

Figure 7. Inhibition of intrahepatic inflammation by JAK2 antagonist TG101348 (TG) in acute CCl4-induced liver injury mouse model. *A*) Representative photomicrographs showing F4/80 (pan macrophage marker), MHC-II (M1 marker), and β-N-acetyl hexosaminidase (YM-1) (M2 marker)–stained liver sections from control mice and CCl_4-treated mice with and without TG101348. *B*) Quantitative gene expression analysis of iNOS (M1 marker) and arginase (M2 marker) in control mice and CCl_4-treated mice with and without TG101348. *C*) Serum ALT levels (units per milliliter) as measured in control mice and CCl_4-treated mice with and without TG101348. Scale bars, 1mm. $^*P < 0.05$, $^{**}P < 0.01$, $^{***}P < 0.001$ denote significance.

alcoholic liver diseases. To date, most of the studies have used a nonselective JAK2 inhibitor (*i.e.*, AG490), whereas, in the present study, we have demonstrated the role of selective JAK2 antagonist TG101348, further confirming the effects are mainly mediated *via* JAK2. In the present study, we have highlighted the role of JAK2 kinase in inflammatory macrophages (Kupffer cells) in the liver and implication of JAK2 inhibition resulting in reduced inflammatory markers *in vitro* and inhibited macrophage activation in a 3D-spheroids NASH model and intrahepatic inflammation *in vivo.*

In conclusion, in the present work, we have shown the role of the JAK2 pathway in HSCs, inflammatory macrophages, and in liver fibrogenesis. Furthermore, we demonstrated selective inhibition of JAK2 using TG101348, significantly blunted HSCs activation and macrophage-driven inflammation *in vitro in vivo* in an acute liver injury mouse model and in a human 3D-spheroids NASH model. This study therefore suggests that selective inhibition of the JAK2 pathway is a promising therapeutic strategy to inhibit inflammatory and fibrotic diseases. FJ

ACKNOWLEDGMENTS

The authors thank B. Klomphaar (University of Twente, The Netherlands) for technical assistance during the animal

experiments. This project was supported by The Netherlands Organization for Health Research and Development (ZonMw; NWO) Veni Grant 916.151.94 (to R.B.). The authors declare no conflicts of interest.

AUTHOR CONTRIBUTIONS

R. Bansal designed research; B. O. Akcora, E. Dathathri, A. Ortiz-Perez, A. V. Gabriël, and R. Bansal performed research and analyzed the data; E. Dathathri and R. Bansal wrote the paper; and G. Storm and J. Prakash read the manuscript and contributed the resources for conducting this study.

REFERENCES

1. Friedman, S. L. (2008) Mechanisms of hepatic fibrogenesis. *Gastroenterology* **134**, 1655–1669
2. Schuppan, D., and Afdhal, N. H. (2008) Liver cirrhosis. *Lancet* **371**, 838–851
3. Hinz, B. (2007) Formation and function of the myofibroblast during tissue repair. *J. Invest. Dermatol.* **127**, 526–537
4. Hinz, B., Phan, S. H., Thannickal, V. J., Galli, A., Bochaton-Piallat, M. L., and Gabbiani, G. (2007) The myofibroblast: one function, multiple origins. *Am. J. Pathol.* **170**, 1807–1816
5. Akcora, B. O., Storm, G., and Bansal, R. (2018) Inhibition of canonical WNT signaling pathway by β-catenin/CBP inhibitor ICG-001 ameliorates liver fibrosis in vivo through suppression of stromal CXCL12. *Biochim. Biophys. Acta Mol. Basis Dis.* **1864**, 804–818
6. Ju, C., and Tacke, F. (2016) Hepatic macrophages in homeostasis and liver diseases: from pathogenesis to novel therapeutic strategies. *Cell. Mol. Immunol.* **13**, 316–327
7. Tacke, F. (2017) Targeting hepatic macrophages to treat liver diseases. *J. Hepatol.* **66**, 1300–1312
8. Wynn, T. A., and Vannella, K. M. (2016) Macrophages in tissue repair, regeneration, and fibrosis. *Immunity* **44**, 450–462
9. Bansal, R., van Baarlen, J., Storm, G., and Prakash, J. (2015) The interplay of the Notch signaling in hepatic stellate cells and macrophages determines the fate of liver fibrogenesis. *Sci. Rep.* **5**, 18272
10. O'Shea, J. J., Schwartz, D. M., Villarino, A. V., Gadina, M., McInnes, I. B., and Laurence, A. (2015) The JAK-STAT pathway: impact on human disease and therapeutic intervention. *Annu. Rev. Med.* **66**, 311–328
11. Gao, B. (2005) Cytokines, STATs and liver disease. *Cell. Mol. Immunol.* **2**, 92–100
12. Granzow, M., Schierwagen, R., Klein, S., Kowallick, B., Huss, S., Linhart, M., Mazar, I. G., Görtzen, J., Vogt, A., Schildberg, F. A., Gonzalez-Carmona, M. A., Wojtalla, A., Krämer, B., Nattermann, J., Siegmund, S. V., Werner, N., Fürst, D. O., Laleman, W., Knolle, P., Shah, V. H., Sauerbruch, T., and Trebicka, J. (2014) Angiotensin-II type 1 receptor-mediated Janus kinase 2 activation induces liver fibrosis. *Hepatology* **60**, 334–348
13. Klein, S., Rick, J., Lehmann, J., Schierwagen, R., Schierwagen, I. G., Verbeke, L., Hittatiya, K., Uschner, F. E., Manekeller, S., Strassburg, C. P., Wagner, K. U., Sayeski, P. P., Wolf, D., Laleman, W., Sauerbruch, T., and Trebicka, J. (2017) Janus-kinase-2 relates directly to portal hypertension and to complications in rodent and human cirrhosis. *Gut* **66**, 145–155
14. Shi, S. Y., Martin, R. G., Duncan, R. E., Choi, D., Lu, S. Y., Schroer, S. A., Cai, E. P., Luk, C. T., Hopperton, K. E., Domenichiello, A. F., Tang, C., Naples, M., Dekker, M. J., Giacca, A., Adeli, K., Wagner, K. U., Bazinet, R. P., and Woo, M. (2012) Hepatocyte-specific deletion of Janus kinase 2 (JAK2) protects against diet-induced steatohepatitis and glucose intolerance. *J. Biol. Chem.* **287**, 10277–10288
15. Themanns, M., Mueller, K. M., Kessler, S. M., Golob-Schwarzl, N., Mohr, T., Kaltenecker, D., Bourgeais, J., Paier-Pourani, J., Friedbichler, K., Schneller, D., Schlederer, M., Zebedin-Brandl, E., Terracciano, L. M., Han, X., Kenner, L., Wagner, K. U., Mikulits, W., Kozlov, A. V., Heim, M. H., Gouilleux, F., Haybaeck, J., and Moriggl, R. (2016) Hepatic deletion of Janus kinase 2 counteracts oxidative stress in mice. *Sci. Rep.* **6**, 34719
16. Freitas, M. C., Uchida, Y., Zhao, D., Ke, B., Busuttil, R. W., and Kupiec-Weglinski, J. W. (2010) Blockade of Janus kinase-2 signaling ameliorates mouse liver damage due to ischemia and reperfusion. *Liver Transpl.* **16**, 600–610
17. Mohan, C. D., Bharathkumar, H., Bulusu, K. C., Pandey, V., Rangappa, S., Fuchs, J. E., Shanmugam, M. K., Dai, X., Li, F., Deivasigamani, A., Hui, K. M., Kumar, A. P., Lobie, P. E., Bender, A. Basappa, Sethi, G., and Rangappa, K. S. (2014) Development of a novel azaspirane that targets the Janus kinase-signal transducer and activator of transcription (STAT) pathway in hepatocellular carcinoma in vitro and in vivo. *J. Biol. Chem.* **289**, 34296–34307
18. Shi, S. Y., Luk, C. T., Schroer, S. A., Kim, M. J., Dodington, D. W., Sivasubramaniyam, T., Lin, L., Cai, E. P., Lu, S. Y., Wagner, K. U., Bazinet, R. P., and Woo, M. (2017) Janus Kinase 2 (JAK2) dissociates hepatosteatosis from hepatocellular carcinoma in mice. *J. Biol. Chem.* **292**, 3789–3799
19. Zhang, L., Yang, Z., Ma, A., Qu, Y., Xia, S., Xu, D., Ge, C., Qiu, B., Xia, Q., Li, J., and Liu, Y. (2014) Growth arrest and DNA damage 45G down-regulation contributes to Janus kinase/signal transducer and activator of transcription 3 activation and cellular senescence evasion in hepatocellular carcinoma. *Hepatology* **59**, 178–189
20. Mas, V. R., Maluf, D. G., Archer, K. J., Yanek, K., Kong, X., Kulik, L., Freise, C. E., Olthoff, K. M., Ghobrial, R. M., McIver, P., and Fisher, R. (2009) Genes involved in viral carcinogenesis and tumor initiation in hepatitis C virus-induced hepatocellular carcinoma. *Mol. Med.* **15**, 85–94
21. Dooley, S., and ten Dijke, P. (2012) TGF-β in progression of liver disease. *Cell Tissue Res.* **347**, 245–256
22. Fabregat, I., Moreno-Càceres, J., Sánchez, A., Dooley, S., Dewidar, B., Giannelli, G., and Ten Dijke, P.; IT-LIVER Consortium. (2016) TGF-β signalling and liver disease. *FEBS J.* **283**, 2219–2232
23. Kaltenecker, D., Themanns, M., Mueller, K. M., Spirk, K., Suske, T., Merkel, O., Kenner, L., Luís, A., Kozlov, A., Haybaeck, J., Müller, M., Han, X., and Moriggl, R. (2018) Hepatic growth hormone - JAK2 - STAT5 signalling: metabolic function, non-alcoholic fatty liver disease and hepatocellular carcinoma progression. [E-pub ahead of print] *Cytokine* doi: 10.1016/j.cyto.2018.10.010
24. Atallah, E., and Verstovsek, S. (2009) Prospect of JAK2 inhibitor therapy in myeloproliferative neoplasms. *Expert Rev. Anticancer Ther.* **9**, 663–670
25. Kolodziejczyk, A. A., Zheng, D., Shibolet, O., and Elinav, E. (2019) The role of the microbiome in NAFLD and NASH. *EMBO Mol. Med.* **11**, e9302
26. Elpek, G. O. (2014) Cellular and molecular mechanisms in the pathogenesis of liver fibrosis: an update. *World J. Gastroenterol.* **20**, 7260–7276

Received for publication January 22, 2019.
Accepted for publication April 23, 2019.